# The Interaction of αB-Crystallin with Mature α-Synuclein Amyloid Fibrils Inhibits Their Elongation

Christopher A. Waudby,[†¶] Tuomas P. J. Knowles,[‡] Glyn L. Devlin,[‖] Jeremy N. Skepper,[§] Heath Ecroyd,[††] John A. Carver,[††] Mark E. Welland,[‡] John Christodoulou,[¶] Christopher M. Dobson,[†] and Sarah Meehan[†*]

[†]University Chemical Laboratory, [‡]Nanoscience Centre, and [§]Department of Physiology, Development and Neuroscience, University of Cambridge, Cambridge, United Kingdom; [¶]Department of Structural and Molecular Biology, University College London, London, United Kingdom; [‖]Department of Biochemistry and Molecular Biology, Monash University, Clayton, Australia; and [††]School of Chemistry and Physics, University of Adelaide, Adelaide, Australia

ABSTRACT αB-Crystallin is a small heat-shock protein (sHsp) that is colocalized with α-synuclein (αSyn) in Lewy bodies—the pathological hallmarks of Parkinson's disease—and is an inhibitor of αSyn amyloid fibril formation in an ATP-independent manner in vitro. We have investigated the mechanism underlying the inhibitory action of sHsps, and here we establish, by means of a variety of biophysical techniques including immunogold labeling and nuclear magnetic resonance spectroscopy, that αB-crystallin interacts with αSyn, binding along the length of mature amyloid fibrils. By measurement of seeded fibril elongation kinetics, both in solution and on a surface using a quartz crystal microbalance, this binding is shown to strongly inhibit further growth of the fibrils. The binding is also demonstrated to shift the monomer-fibril equilibrium in favor of dissociation. We believe that this mechanism, by which a sHsp interacts with mature amyloid fibrils, could represent an additional and potentially generic means by which at least some chaperones protect against amyloid aggregation and limit the onset of misfolding diseases.

## INTRODUCTION

Parkinson's disease (PD) is a progressive neurodegenerative movement disorder distinguished neuropathologically by the presence of Lewy bodies and Lewy neurites—proteinaceous cytoplasmic inclusions—in dopaminergic neurons of the *substantia nigra* (1). Electron microscopy shows these inclusions to be composed of amyloid-like fibrillar material, the major component of which is the 140-residue, intrinsically disordered protein α-synuclein (αSyn) (2). Recombinant αSyn has been found to form aggregates in vitro with all the characteristics of amyloid fibrils associated with diseased states (3). Although most cases of PD are idiopathic, a small number of familial forms have been identified including the A53T variant, in which aggregation is significantly accelerated relative to the wild-type (WT) (4), thus implicating αSyn aggregation in the etiology of PD. As αSyn knockout mice do not exhibit PD-like symptoms, it can be concluded that PD results from a pathological gain of function (i.e., aggregate toxicity) rather than the loss of normal αSyn function (5).

The aggregation mechanism itself, in common with other amyloid systems, is a nucleated process in which there is slow and initially unfavorable association of monomers into a structure competent to elongate into full-length fibrils (6). An important experimental consequence of such a nucleation-polymerization mechanism is the phenomenon of seeding, in which a substoichiometric quantity of preformed fibrils can greatly accelerate the aggregation reaction by bypassing the nucleation process. The aggregation kinetics of seeded reactions are therefore determined only by the elongation and fragmentation rates, and, in the initial rate approximation, by the elongation rate alone (7).

αSyn aggregation may be suppressed by the molecular chaperone Hsp70, and biophysical investigations have shown that this inhibition occurs via binding to prefibrillar species rather than monomeric αSyn (8). Another molecular chaperone that inhibits αSyn aggregation is αB-crystallin, a 175-residue protein ubiquitous in mammalian tissue (9). Early work showed that αB-crystallin is a member of the family of small heat shock proteins (sHsps), and is upregulated in response to a range of stress stimuli and clinical disorders including Alzheimer's disease, transmissible spongiform encephalopathies, dementia with Lewy bodies, and Parkinson's disease (10). As a sHsp, αB-crystallin is a molecular chaperone and has been demonstrated to suppress thermally induced aggregation of β- and γ-crystallins, suggesting that it acts as a significant protective mechanism against cataract formation in the eye lens (11); the latter is associated with aggregation and has been shown in some cases to involve amyloid formation (12). αB-Crystallin also inhibits the aggregation of several other proteins in vitro, including the amyloid-β peptides, $\beta_2$-microglobulin, and insulin (13,14). There are, however, conflicting reports as to whether such inhibition is neuroprotective (15,16).

The sequence of αB-crystallin has amphipathic character, and contains a hydrophobic N-terminal domain, a central α-crystallin domain (common to all sHsps), and a hydrophilic

*Submitted August 3, 2009, and accepted for publication October 1, 2009.*

*Correspondence: sm421@cam.ac.uk



Editor: Heinrich Roder.



0006-3495/10/03/0843/9 $2.00

doi: 10.1016/j.bpj.2009.10.056

and flexible 12-residue C-terminal extension (9). The amphipathic nature of the sequence is believed to be crucial to its chaperone function, enabling αB-crystallin to bind to exposed hydrophobic patches characteristic of misfolded states (17). The hydrophilic and highly flexible C-terminal extension, as characterized by solution state nuclear magnetic resonance (NMR) (18), is also essential to efficient chaperone activity, with an important role in solubilizing complexes of the chaperone with misfolded and aggregated species (10). No crystal structure of αB-crystallin has yet been determined; comparison of the α-crystallin domain with structures of other sHsps, however, suggests that the central domain will adopt a β-sandwich structure (19). A major barrier to structural characterization of αB-crystallin, and certainly to its crystallization, is the self-association of monomers into large, polydispersed assemblies (typically 24–33mers), with molecular masses varying from 300 kDa to >1 MDa (20). Studies of the quaternary structure of the protein by cryo-electron microscopy reveal spherical assemblies between 8 and 18 nm in diameter with a central cavity (21), which undergo subunit exchange on a timescale of minutes (22). This exchange is inhibited by binding to large denatured or partially unfolded proteins, suggesting that subunit exchange may have an important role in the mechanism of chaperone action (10,22).

αB-Crystallin accumulates in neurons and glia of the central nervous system under pathological conditions (23), becoming colocalized with αSyn in Lewy bodies along with a host of other proteins including the sHsp Hsp27, and other chaperones such as clusterin, Hsp70, and Hsp90 (24). In vitro biophysical studies demonstrated complete inhibition of the nucleated assembly of αSyn into fibrils by 0.25 equivalents of αB-crystallin (25). Imaging studies of the aggregation products showed large amounts of amorphous material, which was interpreted as the binding of αB-crystallin to monomeric or oligomeric intermediates, inhibiting the nucleation of fibrillar αSyn aggregates. Later studies additionally demonstrated that the addition of 0.5 equivalents of αB-crystallin to aggregating samples of αSyn is highly effective in inhibiting further growth, and this was also interpreted as a consequence of the stabilization of monomeric or prefibrillar αSyn, inhibiting its incorporation into the growing fibril (26).

Given the complex mechanisms of amyloid formation and the number of aggregated species involved—e.g., monomers, oligomers, protofibrils, fibrils, and amorphous assemblies—we were motivated to consider the interaction of αB-crystallin with additional species along the aggregation pathway and, in particular, with the mature fibrils themselves, which hitherto have largely been regarded as inert reaction products. There is evidence, however, that this view might not be correct, as αB-crystallin has been reported to bind to Aβ40 fibrils, and it has been suggested that this interaction may inhibit further aggregation (13), although the experimental data reported could not conclusively distinguish between the effects of the chaperone in solution or bound to the fibril. A separate study of insulin aggregation at low pH demonstrated that fibril elongation is inhibited after the incubation of the insulin fibrils with αB-crystallin, where the detection of binding stimulated the proposal that the latter serves to limit further fibril growth (14). Here we investigate the hypothesis that αB-crystallin might bind to αSyn fibrils, and use a variety of techniques including newly developed QCM and NMR methodologies to explore the range of effects that result from such chaperone-fibril interactions.

## MATERIALS AND METHODS

These are described in the Supporting Material.

## RESULTS

### Characterization of αSyn interactions with αB-crystallin

The cosedimentation of αB-crystallin and two control proteins (green fluorescent protein, GFP, and ubiquitin hydrolase, UCH-L3) with preformed A53T αSyn fibrils was assayed by SDS-PAGE (Fig. 1 *A*). A53T αSyn was chosen for this study because of its high aggregation propensity relative to the WT protein (4), and it was found to pellet αB-crystallin in a similar manner to that previously observed for the WT (25). The intensity of staining with Coomassie blue was used to estimate the amount of αB-crystallin present in the pelleted fraction (Fig. S1 *A* in the Supporting Material), and an approximate binding ratio of 0.6:1 αB-crystallin:αSyn was determined, where the latter refers to the concentration of the constituent monomers within the fibrils and the observed staining intensity was normalized by protein mass. The corresponding binding ratios for GFP and UCH-L3 were 0.1:1 and 0.01:1, respectively, both consistent with residual material expected from the incomplete washing of the pellet, and indicating that the sedimentation of αB-crystallin was not due to any generic affinity of proteins for hydrophobic patches on the fibril surface, or rheological effects from the fibril network during centrifugation. αB-Crystallin alone was not observed to sediment under these conditions (Fig. S1, *B* and *C*).

The intrinsic tryptophan fluorescence of αB-crystallin was used to estimate the concentration of the protein remaining in solution after incubation with preformed A53T fibrils and centrifugation for 30 min at 16,000 × *g* (Fig. 1 *B*); these conditions were found sufficient to pellet αSyn fibrils completely, and as αSyn does not contain any tryptophan residues, it exhibits little intrinsic fluorescence. Only a small (6%) though reproducible enhancement of αB-crystallin fluorescence was detected in the presence of monomeric αSyn (Fig. 1 *B*), with a concomitant blue-shift of 1 nm (343–342 nm) indicative of the fluorophore being in a more hydrophobic environment, and consistent with the existence of a weak interaction between αB-crystallin and monomeric αSyn (25).

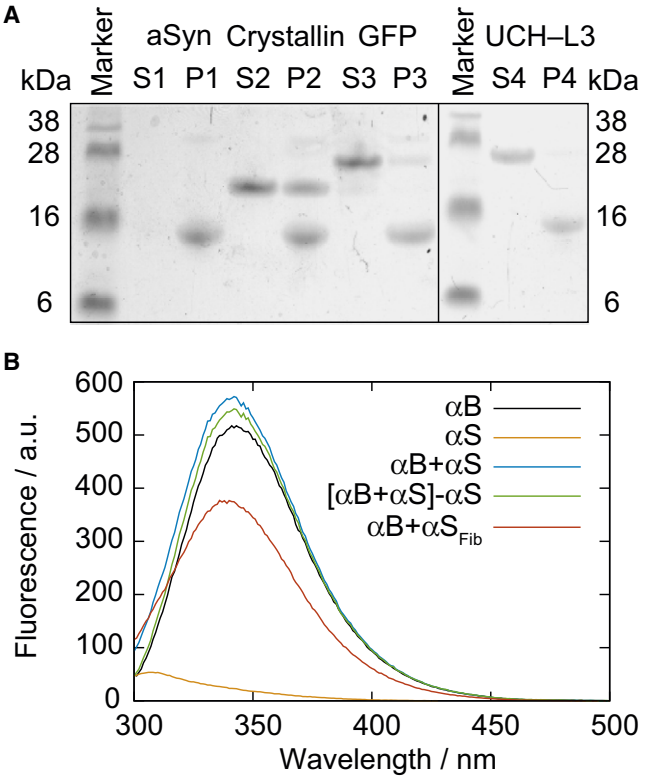


FIGURE 1 Characterization of interactions between αB-crystallin and αSyn. (*A*) SDS-PAGE assay of the binding of αB-crystallin, GFP, and UCH-L3 (all 50 μM) to αSyn fibrils (70 μM), showing both soluble fractions, *S*, and pelleted fractions, *P*, after centrifugation for 30 min at 16,000 × *g*. (*B*) Intrinsic fluorescence of solutions containing αB-crystallin (35 μM) and/or αSyn monomer (35 μM). The spectrum of αSyn monomer alone has also been subtracted from that of αB-crystallin + αSyn to illustrate the 6% enhancement of αB-crystallin fluorescence observed in the presence of αSyn ([αB + αS] − αS). Additionally, a spectrum of αB-crystallin remaining in solution after centrifugation with 0.5 equivalence of αSyn fibrils is presented (αB + $\alpha S_{Fib}$).

To investigate its putative interaction with monomeric αSyn further, αB-crystallin was titrated into uniformly $^{15}$N-labeled αSyn, and changes in the amide chemical shifts were monitored by recording [$^{1}$H,$^{15}$N]-HSQC experiments (Fig. S2). Few significant changes were observed, and the largest perturbation, at His$^{50}$, can be attributed to its high sensitivity to small changes in pH, an observation noted previously in titrations of monomeric αSyn (8). A small, uniform increase in signal intensity was observed, in contrast to previous reports of a uniform loss of intensity (25). This finding suggests that these changes are more probably attributable to the effect of slight pH changes on amide exchange broadening than to the association of αSyn and αB-crystallin. Thus, whereas measurements of tryptophan fluorescence imply that some interaction exists between the proteins, the NMR results reported both here and previously (25) together suggest that this is only transient and of low affinity, similar perhaps to that characterized between αB-crystallin and the amyloid-β peptide (27). For these reasons, these interactions have not been explored further in this work.

The fluorescence assay was then used to measure the concentration of αB-crystallin remaining in solution after precipitation by the addition of αSyn fibrils at two concentrations. A precise determination of the stoichiometry or affinity of the interaction between the sHsp and fibrils is complicated by the effect of the interaction of αSyn monomer with αB-crystallin, as discussed above, and Rayleigh scattering resulting from the small number of αSyn fibrils that remain in solution after centrifugation. In addition, allowance had to be made for the effect of αB-crystallin on the monomer-fibril equilibrium (discussed later) and hence on the absolute fibril concentration. For these reasons, an exact analysis has not been attempted, but it was observed that binding is proportional to the fibril concentration, and an approximate ratio of 0.23 ± 0.06 bound αB-crystallin monomers per αSyn monomer was calculated. This value is expected to be a lower bound, with an absolute uncertainty greater than the quoted standard deviation of the observations, because of the factors discussed above. It is, however, of a comparable order of magnitude to that estimated by densitometry (Fig. S1 *A*).

The binding ratios determined above may be restated in terms of the available fibril surface area, using a toy model (described in Materials and Methods; see Supporting Material) in which the αB-crystallin-fibril interaction is approximated as hard spheres of αB-crystallin monomers packing onto a cylindrical fibril surface. Although there is evidence that the active subunits of αB-crystallin may be dimeric (28), provided that both monomers within any such dimers interact with the fibril surface, we expect that this simple model of monomeric binding will remain approximately applicable. Such an analysis determines an approximate maximum binding ratio of 0.90 ± 0.29 αB-crystallin monomers per αSyn monomer, hence the values determined by fluorescence and densitometry correspond to surface coverages of approximately 26 ± 11% and 62 ± 20%, respectively. Such high values require that the chaperone must bind to the overall surface of the αSyn fibrils, and not just to the small number of fibril ends.

## Inhibition of fibril elongation observed by in situ ThT fluorescence

Previous studies have examined the effect of αB-crystallin on the sigmoidal kinetics characteristic of nucleated polymerization (and fragmentation) reactions associated with the conversion of αSyn into amyloid fibrils (25,26). Such reactions are typically highly stochastic, however, and their quantitative interpretation in terms of individual microscopic processes and rates is complex (7). To simplify the kinetic analysis in this work, preformed fibrils were used to seed the aggregation reaction in order that the elongation step alone could be examined. A series of seeded aggregation

experiments were performed in which the initial elongation velocities were determined as a function of the concentration of αB-crystallin (Fig. 2 *A*). These data show clearly that fibril growth was inhibited at low micromolar concentrations of αB-crystallin. Fitting to a sigmoidal dose-response curve determined the $IC_{50}$ (the concentration of αB-crystallin for half-maximal inhibition) to be 335 ± 86 nM, although some dependence on the seed concentration may also be discerned, which shall be discussed later in this article.

To identify whether or not the inhibition observed above resulted from the binding of chaperone to αSyn in fibrils or free in solution, fibrils were preincubated with αB-crystallin then pelleted, washed, resuspended, and used to seed solutions of monomeric αSyn. Fig. 2 *B* plots the resultant kinetic profiles, and shows that elongation of chaperone-bound fibrils was significantly inhibited (~70-fold) relative to untreated fibrils, by analysis of the initial rates. The residual concentration of αB-crystallin after pelleting and washing was estimated to be ≤35 nM. This is an order-of-magnitude below the $IC_{50}$ and therefore not by itself sufficient to inhibit elongation, as indicated by the marker in Fig. 2 *A*. We therefore conclude that the observed inhibition of elongation results from the specific interaction of αB-crystallin with the αSyn seed fibrils.

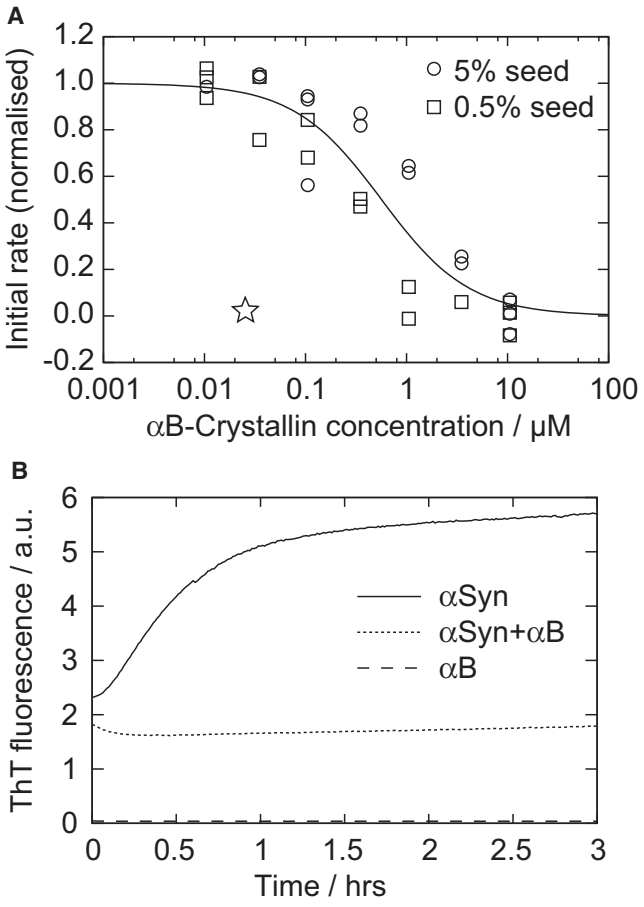


FIGURE 2 Effect of αB-crystallin on αSyn aggregation kinetics. (*A*) Determination of the effective αB-crystallin concentration required for inhibition of seeded fibril elongation in the presence of 35 μM αSyn monomer, as a function of varying fibril mass, given as the % seed. Data were globally fitted to a one-site binding model as described in Materials and Methods (see Supporting Material). Initial rates have been normalized to αSyn elongation in the absence of αB-crystallin. The marker (☆) indicates the relative inhibition resulting from the preincubation of the fibril seed with αB-crystallin, observed in Fig. 2 *B*, given that the estimated residual concentration of αB-crystallin was <35 nM. (*B*) Seeded elongation kinetics, monitored by in situ ThT fluorescence. Samples containing 70 μM αSyn fibrils and/or 70 μM αB-crystallin, as indicated in the legend, were pelleted, washed, and resuspended, then used to seed fresh αSyn monomer (35 μM, 5% w/w seed, 20 μM ThT).

## Inhibition of fibril elongation observed with a quartz crystal microbalance

To verify the model of inhibition discussed above, an independent technique utilizing a quartz crystal microbalance (QCM) was employed. QCM is a technique in which the mass deposited on the surface of a quartz crystal oscillator may be determined directly via measurement of the frequency of oscillation, and recently the method has been applied to the study of amyloid growth by measuring the change in mass of growing fibrils attached to the surface (14). Importantly, this technique enables us to examine the elongation phase of fibril growth in isolation to other processes such as nucleation, and this has been used to determine the elongation kinetics of insulin fibrils grown at low pH, demonstrating the inhibition of their elongation by αB-crystallin (14). In contrast to insulin fibrils, αSyn fibrils did not adsorb directly onto the sensor surface, and instead were covalently attached via lysine side chains, as described in Materials and Methods (see Supporting Material). A surface prepared in this manner is shown in Fig. 3 *A*, and the fibrils were observed to reproducibly elongate when incubated with monomeric αSyn (Fig. 3 *B*). Elongation was readily determined to be proportional to the monomer concentration (Fig. S3), as previously observed by solution-state measurements (6), implying that the presence of the surface does not significantly alter the elongation mechanism.

Fig. 3 *C* plots the change in deposited mass during a single QCM experiment. This shows firstly the increase in mass that results from the elongation of αSyn fibrils in the presence of αSyn monomer (*arrow* 1). The subsequent injection of αB-crystallin with αSyn monomer (*arrow* 2) resulted in a large increase in mass indicative of a binding interaction. After 10 min, the reaction chamber was washed thoroughly with buffer to eliminate unbound chaperone, yet upon the injection of fresh αSyn monomer (*arrow* 3), further elongation was inhibited approximately sevenfold. As no free αB-crystallin remained in solution, inhibition must have resulted from the persistent binding of the chaperone to fibrils, providing strong support for the solution-state inhibition results presented previously in Fig. 2.

A second experiment (Fig. 3 *D*) confirmed this observation: on injection of αSyn and αB-crystallin, a large initial

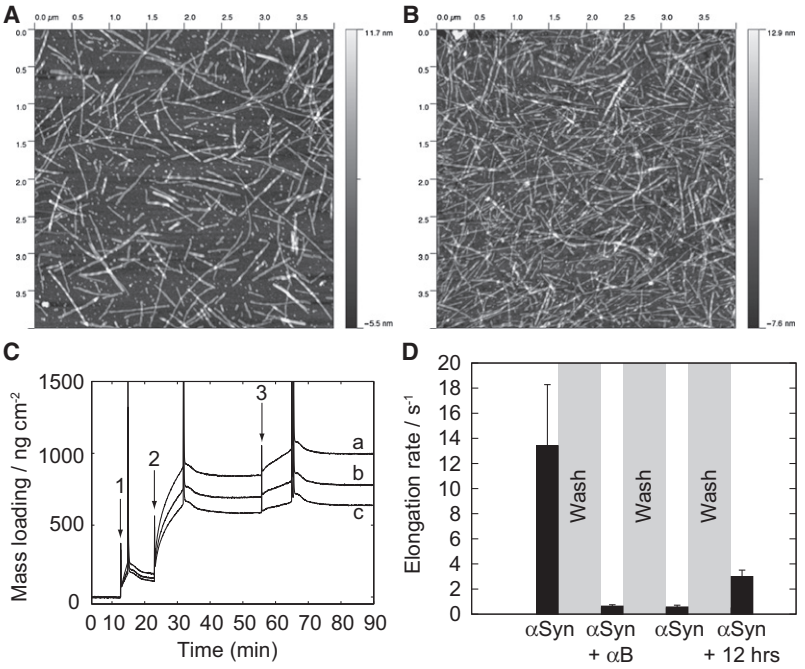


FIGURE 3 Measurement of fibril elongation by QCM. AFM imaging of the (*A*) preparation and (*B*) growth of αSyn fibrils on an activated gold surface. (*C*) The effect of αB-crystallin on fibril elongation, studied by QCM. Mass loading plot showing mass changes calculated from the (*a*) third, (*b*) fifth, and (*c*) seventh harmonics of the crystal. Arrows indicate injection of 1), 0.25 mg/mL A53T; 2), 0.25 mg/mL A53T plus 0.18 mg/mL αB-crystallin; and 3), 0.25 mg/mL A53T, showing approximately sevenfold inhibition of elongation. (*D*) Elongation rates determined in a separate QCM experiment, where αSyn monomer was injected at 0.1 mg/mL in the absence or presence of αB-crystallin at 0.5 mg/mL, as labeled on the *x* axis. The reaction chamber was flushed with fresh buffer between measurements. As in Fig. 3 *C*, on injection of αB-crystallin and αSyn, a large increase in mass loading occurred over ~0.5 h, after which linear growth was observed, and the elongation rate is plotted for this steady-state condition. The final measurement of elongation was performed after overnight incubation of the surface in fresh buffer.

increase in mass loading was detected. In contrast to the previous experiment, this binding was allowed to saturate, and after ~30 min a small but constant elongation rate was observed. It is perhaps noteworthy that this timescale for association is of similar magnitude to that for the subunit exchange of αB-crystallin (22), and may indicate that the αB-crystallin subunits are the active chaperone species. Again, the observed inhibition persisted when the reaction chamber was flushed with fresh buffer. After overnight incubation of the crystallin-treated fibrils in fresh buffer, however, the ability of the fibrils to elongate was partially restored, thus demonstrating the reversibility of the fibril-crystallin interaction. But the results also imply that dissociation of the complex occurs only on a timescale of several hours, which is suggestive of a tight binding interaction.

## NMR investigations of the interaction of αB-crystallin with αSyn fibrils

Large species such as amyloid fibrils, with masses of approximately GDa, have traditionally been assumed to be beyond the reach of solution-state NMR methods. Recent investigations have demonstrated, however, that in some cases noncore regions of fibrils have sufficient flexibility to allow us to detect sharp resonances (29). Therefore, in a one-dimensional $^1$H NMR spectrum of αB-crystallin in the presence of αSyn fibrils, there are four components that may potentially be observed: fibrillar αSyn; residual αSyn monomers; monomeric/oligomeric αB-crystallin; and fibril-bound αB-crystallin. Residual monomeric species are key observables in the study of the thermodynamics of polymerization, and measurements designed to estimate this concentration have been used to characterize the energetics of elongation for several fibril-forming systems (30). The $^1$H spectrum of αB-crystallin has previously been characterized, and reveals that in the native oligomeric complex, the final 12 residues in the C-terminal extension have sufficient mobility to be observable by solution-state NMR (18).

Before examination of the fibril-chaperone complex, the spectrum of αSyn fibrils in solution was explored. Fig. 4 *A* shows a portion of the one-dimensional $^1$H NMR spectrum of a solution of αSyn fibrils (*green line*). The fibril spectrum appears almost identical to that of monomeric αSyn (not shown), albeit with significantly reduced intensity. Although this spectrum suggests that the bulk of the observed signal arises from residual monomers in solution rather than the fibrils, a more detailed study was nevertheless carried out using a series of pulsed-field gradient (PFG) measurements to define the effective diffusion coefficient $D_{\mathrm{eff}}$ of the species giving rise to the resonances. For monomeric proteins, $D_{\mathrm{eff}}$ is identical to the translational diffusion coefficient $D_{\mathrm{trans}}$, and its value is independent of the diffusion delay in the NMR experiment, Δ. By contrast, for very large molecular assemblies such as amyloid fibrils, $D_{\mathrm{eff}}$ can include contributions from rotational diffusion such that $D_{\mathrm{eff}} > D_{\mathrm{trans}}$ for small values of Δ (31). $D_{\mathrm{eff}}$ is shown in Fig. S4 as a function of Δ for a solution containing αSyn fibrils, and no such variation was detected. The mean value of $D_{\mathrm{eff}}$ was $8.6(\pm 1.7) \times 10^{-11}$ m$^2$ s$^{-1}$, which is entirely consistent with that expected for a small monomeric protein (32). Thus, in contrast to other amyloid systems such as the SH3 dimer, for which fibril resonances are observable (29), the NMR signal in Fig. 4 *A* may be attributed to residual αSyn monomers alone.

Having examined the spectrum of isolated αSyn fibrils (in equilibrium with residual monomer), it is then possible to analyze their interaction with αB-crystallin. Fig. 4 *A* shows

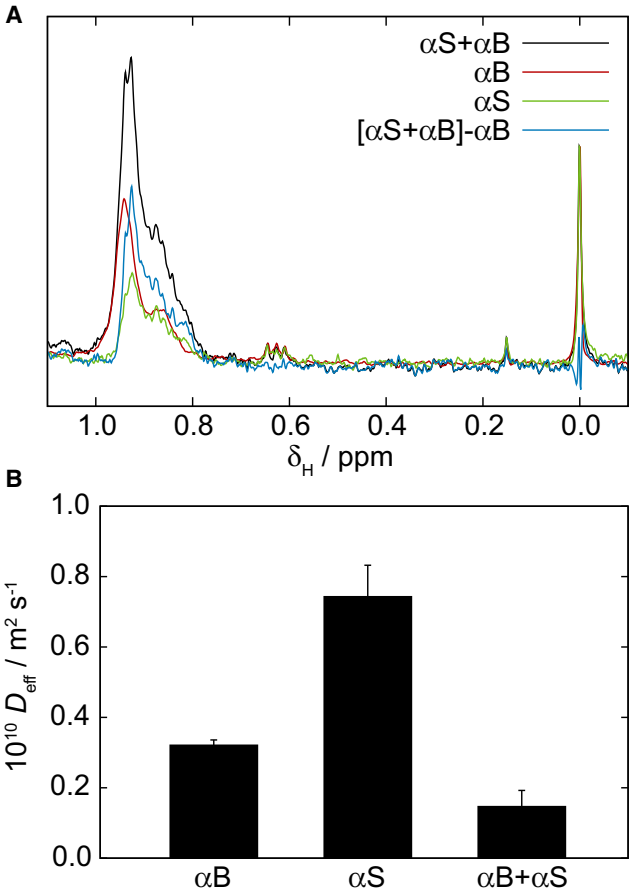


FIGURE 4 Interaction of αB-crystallin with αSyn fibrils observed by one-dimensional $^1$H NMR spectroscopy. (*A*) Methyl and DSS (resonance at 0 ppm) regions of the one-dimensional $^1$H spectra of 70 μM A53T αSyn fibrils complexed with 20 μM αB-crystallin, and of the fibrils and chaperone separately. (*B*) Effective diffusion coefficients determined for these samples by PFG NMR experiments using a 500-ms diffusion delay.

the methyl region of the one-dimensional $^1$H NMR spectrum of the fibril-crystallin complex alongside spectra of each component in isolation. Difference spectroscopy, normalized using the internal DSS reference, reveals that the spectrum of chaperone-bound fibrils is not the sum of the original components, but that there is additional signal in the spectrum of the complex. The difference spectrum had, however, the same appearance as monomeric αSyn (Fig. 4 *A*). A comparison of intensities in repeated experiments using independent fibril samples determined that the mean αSyn intensity in the presence of αB-crystallin is ~50% greater than that in its absence.

To investigate these results further, PFG NMR spectra were recorded to characterize the diffusion properties of the observed resonances. To limit the contributions from rotational motion to the diffusion coefficients measured for fibril-associated species, a long (500-ms) diffusion period Δ was employed (31). The effective diffusion coefficients $D_{\mathrm{eff}}$ for each sample are plotted in Fig. 4 *B* and these data show that the diffusion of αB-crystallin is retarded in the presence of αSyn fibrils, consistent with the formation of a fibril-chaperone complex. The measured diffusion coefficients correspond, according to the Stokes-Einstein relation, to approximate hydrodynamic radii of 3.7 ± 0.4 nm and 8.6 ± 0.4 nm for free αSyn and αB-crystallin, respectively—in good agreement with previous observations (21,33). The effective diffusion coefficient of αB-crystallin in the presence of αSyn fibrils corresponds, when modeled as rotating rigid rods (31), to a mean fibril length of 260 ± 140 nm.

The simplest interpretation of these results is that the C-terminal extension of αB-crystallin is not perturbed by fibril binding and remains free to tumble in solution; hence, the one-dimensional NMR spectrum is not altered in the presence of fibrils. However, diffusion is retarded, a finding consistent with the binding of αB-crystallin to the fibrils. The concentration of residual αSyn monomer is also increased in the presence of αB-crystallin, indicating that the monomer-fibril equilibrium is perturbed by interactions with the chaperone. Although absolute concentrations of αSyn monomer were not determined, the observed 50% increase in the monomer concentration corresponds to a net destabilization of 0.3 ± 0.1 kcal mol$^{-1}$ in the free energy of fibril elongation, assuming a simple polymerization model (30). It is recognizable that the chaperone-monomer-fibril system comprises many coupled equilibria, and that there are potentially multiple origins to the observed increase in monomer concentration. It remains, however, a notable feature of polymerization reactions that a relatively small change in the net elongation energy may still result in a large change in the partition of monomers and fibrils.

## Imaging of the fibril-chaperone complex

To confirm the binding of αB-crystallin to αSyn fibrils in a more direct manner, immunoelectron microscopy was employed to visualize the fibril-crystallin complex. αSyn fibrils are of sufficient size that their twisted ultrastructure could be observed clearly in the electron microscope after negative staining with uranyl acetate (Fig. 5 *A*). In contrast, the αB-crystallin oligomers are more difficult to distinguish, particularly in a multicomponent system. Samples were therefore incubated with an antibody directed against αB-crystallin, which was in turn stained with a secondary antibody conjugated to 10-nm gold nanoparticles. Fig. 5 *B* shows a sample of αB-crystallin prepared in this manner and negatively stained with uranyl acetate; electron dense gold nanoparticles are observed to be colocalized with the native αB-crystallin assemblies. The αSyn fibrils shown in Fig. 5 *A* were also stained with the primary and secondary antibodies by an identical protocol; no significant nonspecific or background immunolabeling was observed. An immunolabeled fibril-crystallin complex containing 0.3 equivalents of αB-crystallin was then imaged (Fig. 5 *C*), showing, very clearly, the interaction of αB-crystallin along the length of the fibrils,

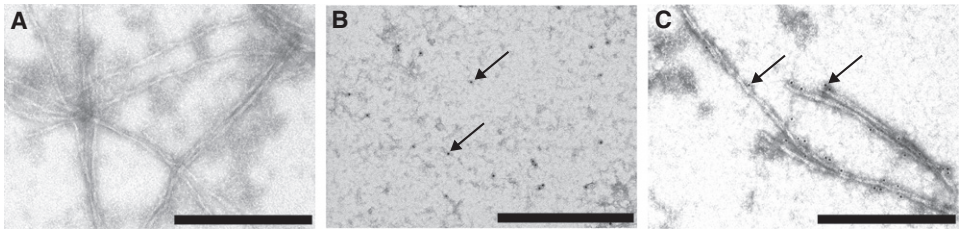


FIGURE 5 Immunoelectron microscopy of αB-crystallin-αSyn fibril complexes. αB-Crystallin was labeled with 10-nm gold nanoparticles (*arrows*) as described in Materials and Methods (see Supporting Material). (*A*) αSyn fibrils alone; (*B*) αB-crystallin alone; and (*C*) αSyn fibrils plus 0.3 equivalence of αB-crystallin. All scale bars are 500 nm.

with gold nanoparticles observed on all faces of the fibril surface including occasional binding at the fibril ends.

## DISCUSSION

The results of this article have enabled a novel mechanism to be proposed for the inhibition of αSyn aggregation by the small heat-shock protein αB-crystallin. αB-Crystallin has been demonstrated to bind along the lateral surface of αSyn amyloid fibrils, and this interaction has been demonstrated by a range of methods to inhibit elongation effectively, with half-maximal inhibition at an αB-crystallin concentration of 335 ± 86 nM. Although the binding epitopes of αB-crystallin and the fibrils are unknown, NMR investigations have determined that the C-terminal extension of αB-crystallin is able to fluctuate freely even in the bound state, a finding consistent with its purported role as a solubilizing domain (18). NMR measurements also indicated that the presence of the chaperone perturbed the monomer-fibril equilibrium, consistent with a net destabilization of the fibrils by ~0.3 kcal $mol^{-1}$. This may indicate that binding of αB-crystallin along αSyn fibrils weakens the interactions between adjacent αSyn molecules, similar to the effect of cofilin binding to actin filaments (34), but the additional effect of a weak interaction between αB-crystallin and monomeric αSyn cannot be ruled out at this stage.

In this work, a novel methodology based on QCM measurements has been developed to monitor αSyn fibril elongation, in isolation from other processes such as nucleation, and without the need for added probe molecules. As has been demonstrated in studies of insulin aggregation (14), this technique offers significant promise for the quantitative investigation of the kinetics and mechanism of αSyn fibril elongation. To apply this, however, methods were developed similar to those used in surface plasmon resonance to enable the gold surface to bind the fibrils. This approach is likely to be applicable to QCM measurements of other amyloid systems that do not contain accessible thiols or disulphides.

αB-Crystallin has previously been reported to inhibit αSyn aggregation, when added even at the midpoint of sigmoidal assembly curves, and it was hypothesized that the chaperone acts by stabilizing monomeric or prefibrillar species (25,26). The mechanism put forward in this study, by which αB-crystallin could inhibit fibril formation by binding to the fibrils and inhibiting their elongation, suggests that there may be multiple mechanisms of chaperone action. As binding is likely to occur at least in part to the hydrophobic clusters that may form in the fibrils, it is likely that αB-crystallin will also interact strongly with the oligomeric precursor species, an important property given their cytotoxic nature (2).

Two mechanisms can be envisaged to rationalize the inhibition of elongation that results from the interaction of αSyn fibrils with αB-crystallin: one is a specific capping interaction of αB-crystallin with the fibril ends, assuming that the binding here is tighter than that along the length of the fibril; and the second involves uniform binding of αB-crystallin along the length of the fibril, where inhibition results from the chance occlusion of the fibril ends. In this latter binding and occlusion model, inhibition is expected to be observed only in the presence of near equimolar ratios of αB-crystallin and αSyn fibrils, and the dependence of the $IC_{50}$ upon the seed concentration noted in Fig. 2 *A* would be consistent with such a mechanism. Further investigations of the stoichiometry and affinity of the fibril-chaperone interaction will, however, be required to differentiate these models with confidence.

A key question in the study of sHsps is whether the native oligomers act as chaperones directly, or whether dissociation into subunits occurs before their binding (35). The approximate binding ratios presented in this work would be consistent with either a relatively uniform binding of monomeric or dimeric αB-crystallin subunits along the fibril surfaces, or a rarer binding of the oligomers. The high surface coverage that would result from the subunit binding appears attractive as a means of explaining the efficacy of inhibition, particularly as this effect persists when the chaperone is removed from the solution after binding has occurred. Although this mechanism of inhibition has not been put forward previously, it is consistent with previous studies in which sHsp subunit exchange dynamics have been correlated to chaperone activity, in both αB-crystallin and its phosphorylated derivatives (22,36).

These findings present the suggestion that other sHsps may act by a similar mechanism. The Hsp20 from the bovine parasite *Babesia bovis* inhibits Aβ40 amyloid formation, and the chaperone was active only at low (10–100 nM) concentrations in which dimeric subunits were prevalent, whereas at higher chaperone concentrations, in which larger

oligomers became populated, the inhibition of aggregation was no longer observed (37). Additionally, αB-crystallin may bind to components of the cytoskeleton including intermediate filaments and microtubules, although electron microscopy has demonstrated that such binding occurs via the oligomeric complex rather than isolated subunits (38). This suggests that different chaperone activities (e.g., suppressing amyloid formation, thermally induced amorphous aggregation, and cytoskeletal binding) correspond to a variety of phosphorylation or oligomerization states and binding modes. For example, lysozyme unfolding intermediates are bound by multimeric Hsp27 (39), and whereas αB-crystallin activity against αSyn amyloid formation increases with temperature (correlating with increased subunit exchange), little variation with temperature was observed against the thermally induced amorphous aggregation of alcohol dehydrogenase and citrate synthase (40). Phosphorylation-mimicking mutations have also been demonstrated to differentially regulate the chaperone activity of αB-crystallin against amyloid fibril formation and amorphous aggregation (36). Equally, however, some of this variation may result from a degree of specificity of individual members of the sHsp family (41).

αB-Crystallin has shown no evidence of ATPase or refolding activity (19). Instead, sHsps have been proposed to bind to misfolded states before interaction with other chaperone systems, which may facilitate refolding or degradation (41). Horwitz et al. (9) has suggested that αB-crystallin in the eye lens may act as an irreversible sink for unfolded or misfolded proteins, as there is no evidence of further chaperone systems within the lens, and active protein synthesis does not occur once the lens proteins are laid down. The binding of αB-crystallin to αSyn fibrils may therefore be a protective mechanism to stem the growth of amyloid deposits before clearance by further quality control mechanisms within the cell (41). This hypothesis is supported by a mouse model of PD expressing A53T αSyn, in which selective upregulation of αB-crystallin was observed in affected glial cells (42). Additionally, we suggest that binding of αB-crystallin to fibrils may reduce their cytotoxicity by camouflaging exposed hydrophobic surfaces. This hypothesis is supported by a tissue culture model of Lewy body disease in which colocalization of αB-crystallin with αSyn deposits occurs without a reduction in the number of inclusions compared to cells not transfected with αB-crystallin, although there is a significant reduction in cytotoxicity (43). Finally, as exposed fibril surfaces have been proposed to act as sites of secondary fibril nucleation (44), the coating of αSyn fibrils by αB-crystallin could inhibit not just their elongation but further nucleation processes as well. It is also possible, however, that fibril binding by chaperones may have a deleterious role by sequestering them and reducing their efficacy in other physiological functions, e.g., interacting with misfolded monomers or oligomers, or, indeed, helping in regulation of the cytoskeleton (41). Certainly, these findings reveal novel activities of the cellular proteostasis network, which is of growing interest in the field of systems biology, and an increasing understanding of its behavior may contribute to the rational development of therapeutic proteostasis regulators (45).

This finding is also likely to have general relevance to other amyloid and chaperone systems. Indeed, recent work suggests that another chaperone, Hsp104, is capable of suppressing amyloid growth at many stages along the aggregation pathway, including the elongation of mature fibrils (46). Fibril binding and inhibition of elongation by αB-crystallin has previously been demonstrated for the Aβ40 peptide, although no causal link was demonstrated (13). Inhibition of $\beta_2$-microglobulin elongation by αB-crystallin at low pH was also reported (13), and inhibition of insulin aggregation under similar conditions has also been observed (14). This work is therefore important in extending mechanistic studies of αB-crystallin to physiological conditions and, given apparent similarities in the behavior of αSyn, Aβ40, $\beta_2$-microglobulin, and insulin, suggests a generic mechanism of αB-crystallin action.

## SUPPORTING MATERIAL

Materials and Methods and six figures are available at http://www.biophysj.org/biophysj/supplemental/S0006-3495(09)01741-X.

The authors thank Fredrik Andersson for the gift of UCH-L3. We thank the staff of and acknowledge the use of the Biomolecular NMR Facility, Department of Chemistry, University of Cambridge, and support from the Multi-Imaging Centre, University of Cambridge.

This work was supported by grants from Unilever and the Biotechnology and Biological Sciences Research Council (to C.A.W.); Engineering and Physical Sciences Research Council and Interdisciplinary Research Council in Nanotechnology (to T.P.J.K. and M.E.W.); National Health and Medical Research Council of Australia, C.J. Martin Fellowship (G.L.D.); National Health and Medical Research Council of Australia, Peter Doherty Fellowship (to H.E.); Australian Research Council (to J.A.C.); Wellcome Trust and Leverhulme Trust (to J.C. and C.M.D.); and a Royal Society Dorothy Hodgkin Fellowship (to S.M.).

## REFERENCES

1. Goedert, M. 2001. Alpha-synuclein and neurodegenerative diseases. *Nat. Rev. Neurosci.* 2:492–501.
2. Cookson, M. R. 2005. The biochemistry of Parkinson's disease. *Annu. Rev. Biochem.* 74:29–52.
3. Serpell, L. C., J. Berriman, …, R. A. Crowther. 2000. Fiber diffraction of synthetic α-synuclein filaments shows amyloid-like cross-β conformation. *Proc. Natl. Acad. Sci. USA.* 97:4897–4902.
4. Conway, K. A., S. J. Lee, …, P. T. Lansbury, Jr. 2000. Acceleration of oligomerization, not fibrilization, is a shared property of both α-synuclein mutations linked to early-onset Parkinson's disease: implications for pathogenesis and therapy. *Proc. Natl. Acad. Sci. USA.* 97:571–576.
5. Abeliovich, A., Y. Schmitz, …, A. Rosenthal. 2000. Mice lacking α-synuclein display functional deficits in the nigrostriatal dopamine system. *Neuron.* 25:239–252.
6. Wood, S. J., J. Wypych, …, A. L. Biere. 1999. Alpha-synuclein fibrillogenesis is nucleation-dependent. Implications for the pathogenesis of Parkinson's disease. *J. Biol. Chem.* 274:19509–19512.

7. Ferrone, F. 1999. Analysis of protein aggregation kinetics. *Methods Enzymol.* 309:256–274.
8. Dedmon, M. M., J. Christodoulou, …, C. M. Dobson. 2005. Heat shock protein 70 inhibits α-synuclein fibril formation via preferential binding to prefibrillar species. *J. Biol. Chem.* 280:14733–14740.
9. Horwitz, J. 2003. Alpha-crystallin. *Exp. Eye Res.* 76:145–153.
10. Sun, Y., and T. H. MacRae. 2005. Small heat shock proteins: molecular structure and chaperone function. *Cell. Mol. Life Sci.* 62:2460–2476.
11. Horwitz, J. 1992. Alpha-crystallin can function as a molecular chaperone. *Proc. Natl. Acad. Sci. USA.* 89:10449–10453.
12. Sandilands, A., A. M. Hutcheson, …, R. A. Quinlan. 2002. Altered aggregation properties of mutant γ-crystallins cause inherited cataract. *EMBO J.* 21:6005–6014.
13. Raman, B., T. Ban, …, ChM. Rao. 2005. αB-crystallin, a small heat-shock protein, prevents the amyloid fibril growth of an amyloid β peptide and β2-microglobulin. *Biochem. J.* 392:573–581.
14. Knowles, T. P. J., W. Shu, …, M. E. Welland. 2007. Kinetics and thermodynamics of amyloid formation from direct measurements of fluctuations in fibril mass. *Proc. Natl. Acad. Sci. USA.* 104:10016–10021.
15. Stege, G. J., K. Renkawek, …, W. W. de Jong. 1999. The molecular chaperone αB-crystallin enhances amyloid-β neurotoxicity. *Biochem. Biophys. Res. Commun.* 262:152–156.
16. Wilhelmus, M. M. M., W. C. Boelens, …, M. M. Verbeek. 2006. Small heat shock proteins inhibit amyloid-β protein aggregation and cerebrovascular amyloid-β protein toxicity. *Brain Res.* 1089:67–78.
17. Reddy, G. B., P. A. Kumar, and M. S. Kumar. 2006. Chaperone-like activity and hydrophobicity of α-crystallin. *IUBMB Life.* 58:632–641.
18. Carver, J. A. 1999. Probing the structure and interactions of crystallin proteins by NMR spectroscopy. *Prog. Retin. Eye Res.* 18:431–462.
19. van Montfort, R. L., E. Basha, …, E. Vierling. 2001. Crystal structure and assembly of a eukaryotic small heat shock protein. *Nat. Struct. Biol.* 8:1025–1030.
20. Aquilina, J. A., J. L. P. Benesch, …, C. V. Robinson. 2003. Polydispersity of a mammalian chaperone: mass spectrometry reveals the population of oligomers in αB-crystallin. *Proc. Natl. Acad. Sci. USA.* 100:10611–10616.
21. Haley, D. A., J. Horwitz, and P. L. Stewart. 1998. The small heat-shock protein, αB-crystallin, has a variable quaternary structure. *J. Mol. Biol.* 277:27–35.
22. Ahmad, M. F., B. Raman, …, C. h. M. Rao. 2008. Effect of phosphorylation on αB-crystallin: differences in stability, subunit exchange and chaperone activity of homo and mixed oligomers of αB-crystallin and its phosphorylation-mimicking mutant. *J. Mol. Biol.* 375:1040–1051.
23. Iwaki, T., T. Wisniewski, …, J. E. Goldman. 1992. Accumulation of αB-crystallin in central nervous system glia and neurons in pathologic conditions. *Am. J. Pathol.* 140:345–356.
24. Wakabayashi, K., K. Tanji, …, H. Takahashi. 2007. The Lewy body in Parkinson's disease: molecules implicated in the formation and degradation of α-synuclein aggregates. *Neuropathology.* 27:494–506.
25. Rekas, A., C. G. Adda, …, J. A. Carver. 2004. Interaction of the molecular chaperone αB-crystallin with α-synuclein: effects on amyloid fibril formation and chaperone activity. *J. Mol. Biol.* 340:1167–1183.
26. Rekas, A., L. Jankova, …, J. A. Carver. 2007. Monitoring the prevention of amyloid fibril formation by α-crystallin. Temperature dependence and the nature of the aggregating species. *FEBS J.* 274:6290–6304.
27. Narayanan, S., B. Kamps, …, B. Reif. 2006. αB-crystallin competes with Alzheimer's disease β-amyloid peptide for peptide-peptide interactions and induces oxidation of AβMet35. *FEBS Lett.* 580: 5941–5946.
28. Aquilina, J. A., J. L. P. Benesch, …, C. V. Robinson. 2004. Phosphorylation of αB-crystallin alters chaperone function through loss of dimeric substructure. *J. Biol. Chem.* 279:28675–28680.
29. Baldwin, A. J., R. Bader, …, P. D. Barker. 2006. Cytochrome display on amyloid fibrils. *J. Am. Chem. Soc.* 128:2162–2163.
30. O'Nuallain, B., A. K. Thakur, …, R. Wetzel. 2006. Kinetics and thermodynamics of amyloid assembly using a high-performance liquid chromatography-based sedimentation assay. *Methods Enzymol.* 413: 34–74.
31. Baldwin, A. J., J. Christodoulou, …, G. Lippens. 2007. Contribution of rotational diffusion to pulsed field gradient diffusion measurements. *J. Chem. Phys.* 127:114505.
32. Wilkins, D. K., S. B. Grimshaw, …, L. J. Smith. 1999. Hydrodynamic radii of native and denatured proteins measured by pulse field gradient NMR techniques. *Biochemistry.* 38:16424–16431.
33. Weinreb, P. H., W. Zhen, …, P. T. Lansbury, Jr. 1996. NACP, a protein implicated in Alzheimer's disease and learning, is natively unfolded. *Biochemistry.* 35:13709–13715.
34. Du, J., and C. Frieden. 1998. Kinetic studies on the effect of yeast cofilin on yeast actin polymerization. *Biochemistry.* 37:13276–13284.
35. Carver, J. A., A. Rekas, …, M. R. Wilson. 2003. Small heat-shock proteins and clusterin: intra- and extracellular molecular chaperones with a common mechanism of action and function? *IUBMB Life.* 55:661–668.
36. Ecroyd, H., S. Meehan, …, J. A. Carver. 2007. Mimicking phosphorylation of αB-crystallin affects its chaperone activity. *Biochem. J.* 401:129–141.
37. Lee, S., K. Carson, …, T. Good. 2005. Hsp20, a novel α-crystallin, prevents Aβ fibril formation and toxicity. *Protein Sci.* 14:593–601.
38. Fujita, Y., E. Ohto, …, Y. Atomi. 2004. αB-Crystallin-coated MAP microtubule resists nocodazole and calcium-induced disassembly. *J. Cell Sci.* 117:1719–1726.
39. Shashidharamurthy, R., H. A. Koteiche, …, H. S. McHaourab. 2005. Mechanism of chaperone function in small heat shock proteins: dissociation of the Hsp27 oligomer is required for recognition and binding of destabilized T4 lysozyme. *J. Biol. Chem.* 280:5281–5289.
40. Reddy, G. B., K. P. Das, …, W. K. Surewicz. 2000. Temperature-dependent chaperone activity and structural properties of human αA- and αB-crystallins. *J. Biol. Chem.* 275:4565–4570.
41. Vos, M. J., J. Hageman, …, H. H. Kampinga. 2008. Structural and functional diversities between members of the human HSPB, HSPH, HSPA, and DNAJ chaperone families. *Biochemistry.* 47:7001–7011.
42. Wang, J., E. Martin, …, M. K. Lee. 2008. Differential regulation of small heat shock proteins in transgenic mouse models of neurodegenerative diseases. *Neurobiol. Aging.* 29:586–597.
43. Outeiro, T. F., J. Klucken, …, P. J. McLean. 2006. Small heat shock proteins protect against α-synuclein-induced toxicity and aggregation. *Biochem. Biophys. Res. Commun.* 351:631–638.
44. Ruschak, A. M., and A. D. Miranker. 2007. Fiber-dependent amyloid formation as catalysis of an existing reaction pathway. *Proc. Natl. Acad. Sci. USA.* 104:12341–12346.
45. Balch, W. E., R. I. Morimoto, …, J. W. Kelly. 2008. Adapting proteostasis for disease intervention. *Science.* 319:916–919.
46. Arimon, M., V. Grimminger, …, H. A. Lashuel. 2008. Hsp104 targets multiple intermediates on the amyloid pathway and suppresses the seeding capacity of Aβ fibrils and protofibrils. *J. Mol. Biol.* 384:1157–1173.